ISSN 0016-7029, Geochemistry International, 2007, Vol. 45, No. 9, pp. 841–856. © Pleiades Publishing, Ltd., 2007.
Original Russian Text © L.N. Kogarko, A.M. Asavin, 2007, published in Geokhimiya, 2007, No. 9, pp. 915–932.

Regional Features of Primary Alkaline Magmas of the Atlantic Ocean

L. N. Kogarko and A. M. Asavin
Vernadsky Institute of Geochemistry and Analytical Chemistry, Russian Academy of Sciences,
ul. Kosygina 19, Moscow, 119991 Russia
e-mail: alex@geokhi.ru

Received December 15, 2006

Abstract—In the framework of the GIS project on the geochemistry of Atlantic intraplate magmatism, primary high-magnesian melts were identified there and subdivided into five types: foidites, picrites, basanite–nephelinites, alkaline olivine basalts, and tholeiite. Their relative proportions were determined for both the Atlantic Ocean as a whole and individual magmatic centers. The compositional ranges and average compositions were calculated. It was shown that alkali rocks are predominant, but tholeiite melts account for about 25%. Among ocean-island volcanic rocks, differentiated varieties clearly dominate over primary melts (80 and 20%, respectively). Variations in the proportions of the distinguished types were applied to prepare a map for the petrochemical typification of Atlantic intraplate magmatism. Seven petrochemical zones were provisionally identified, first demonstrating the lateral petrochemical heterogeneity of intraplate sources of the Atlantic Ocean. In addition to the global heterogeneity, each large center of intraplate magmatism (archipelago or island chain) demonstrates local heterogeneities. The variations in the Na/K, Ti/Na, and Si/Ca ratios reflect significant magma generation depths (in the lower mantle) for intraplate magmatism. It was proposed that variations in the Ti/Na ratio in the high-magnesian melts are controlled by a change in the Na and Ti partition coefficients of pyroxene with increasing magma generation depth. A comparison between evolution of the oceanic and continental alkaline magmatism was conducted.

DOI: 10.1134/S0016702907090017

INTRODUCTION

The trace-element heterogeneity of the upper mantle is presently a very popular idea. To study the upper mantle composition, two approaches are used: (1) studying mantle xenoliths transported by alkali basalts at the surface and (2) using the chemical compositions of primary magmas, the products of partial melting of a mantle protolith. These methods showed a global geochemical (trace element and isotope) heterogeneity of the upper mantle [1–3]. Methods were developed for estimating the size and spatial position of mantle "blocks" with certain characteristics. Events responsible for the isotope heterogeneity of subcrustal zones are dated, and the role of mantle metasomatism in the transfer of ore and rare elements is assessed. Much attention was focused on the geochemical differentiation of subcrustal zones related to the recycling of the oceanic crust. Seismic tomography data [4] showed that subducted material could reach a depth of about 2600 km, i.e., the core–lower mantle boundary layer. The heterogeneity of mantle sources was established most convincingly for ocean islands and mid-ocean ridge basalts [5]. Hast [1] was the first to demonstrate that chemical variations in ocean-floor tholeiites and oceanic-island alkali basalts could not be caused by any variations in the degree of partial melting. Available data on trace element and isotope (U–Pb, Th–Pb, Rb–Sr, Sm–Nd, Lu–Hf) compositions made it possible to recognize two sources of oceanic magmatism [5]. The mantle of mid-ocean ridge basalts (MORB) and the oceanic floor is characterized by a steady decrease of the Rb/Sr, U/Pb, and Th/Pb ratios as compared with chondrites and depletion in incompatible lithophile elements (LREE, Rb, Cs, Ba, Nb, and others). As a result, typical MORB are characterized by $^{143}Nd/^{144}Nd > 0.51305$, $^{87}Sr/^{86}Sr < 0.7030$, $^{206}Pb/^{204}Pb < 18.7$ and subchondritic ratios of Ba/Sr, Cs/Rb, Rb/K, LREE/HREE, and Zr/Nb. The mantle sources of ocean-island alkaline magmatism are, by contrast, enriched in trace lithophile elements and radiogenic isotopes with respect to chondritic primitive mantle. They are characterized by $^{87}Sr/^{86}Sr > 0.7030$, $^{206}Pb/^{204}Pb > 18.7$, and $^{143}Nd/^{144}Nd < 0.51305$, which shows the preservation of ancient mantle reservoirs enriched in incompatible elements.

It was found that mantle sources of MORBs are heterogeneous [5]. For instance, the mantle of Indian MORB is significantly enriched in radiogenic isotopes, which led to the recognition of a DUPAL anomalous zone that occurs mainly in the Southern Hemisphere [6]. However, in general there are two large mantle reservoirs: depleted (source of MORB) and enriched [OIB (within-plate magmatism) source].

This work is aimed at the detailed studying of the geochemical heterogeneity of within-plate magmatism in the ocean as exemplified by the Atlantic. The following problems were considered:

(1) The recognition of the compositional field of alkali volcanic rocks that correspond to primary magmas produced by partial melting of the mantle.

(2) The classification of the primary magmas of ocean islands and seamounts of the Atlantic.

(3) GIS (geographic information systems)-based compilation of maps of petrochemical and geochemical typification of primary melts.

(4) The recognition of petrochemical provinces of within-plate magmatism.

INFORMATION RESOURCES

To solve the problems, we used the database developed since 1989 on the basis of the geochemical cadastre of oceanic islands prepared at the Vernadsky Institute of Geochemistry and Analytical Chemistry, Russian Academy of Sciences, as well as databases available from the Internet ("Petros", IGBA, DSDP, and others). The summarized database involves about 35 thousand records taken from 400 references on 500 occurrences of within-plate magmatism. It should be noted that the database is permanently updated owing to current publications and the retrospective processing of available data, annually increasing by 5–10%. This insignificant increase indicates that the sampling is representative and widely covers available geochemical information on the Atlantic within-plate magmatism. Data were selected based on trace element composition (with limitations on the compositional range), age (geological and direct isotope datings), geography and other geological–structural features, and rock type. The selected data were saved as a DBASE file, and ASCII points were plotted in the Atlantic map Arc/Info v. 8.0. This allows the additional assignment of compositions to the centers of within plate magmatism and the rejection of samples that are plotted in the field of tholeiite magmatism of rift zones and ocean floor, transform faults, and other oceanic structures unrelated with within-plate magmatism. The data were then processed in Arc/View, the program develop and rather widely used in geoinformation studies [7].

Geochemical maps were compiled using a GIS complex developed within the framework of the project "Geodynamic Globe" [8], on a scale of 1 : 10000000, created at the Department of Geoinformation Systems of the Vernadsky State Geological Museum [9] with some additions from individual coverages and special databases of the Vernadsky Institute of Geochemistry and Analytical Chemistry, Russian Academy of Sciences. The sheet of tectonic globe compiled at the VNII Zarubezhgeologiya under the supervision of L.P. Zonenshain in 1995 was used as the cartographic basis [10].

To solve the aforementioned problems, we applied a GIS technology involving a combination of electronic maps with a database. Unlike "conventional" maps, an electronic map provides the following opportunities:

the rapid combination of any thematic maps in a common geographical system;

the comparison of unlimited number of parameters to reveal hidden spatial variations in different values.

To study systematic structural–compositional variations in the within-plate volcanic complexes, we developed the project that involved electronic map coverages, the geoinformation project being the fragment of the Geodynamic Globe. The map of trace element distribution was created using the following technique. Samples selected according to a certain geochemical criteria and element abundances were automatically added to a geoinformation project. Then they were sorted into classes and labeled by circles different in color (or shading) or size. Pie diagrams were used to illustrate the proportions of an element, which are expressed through the size of the sector of corresponding color (shading). To compare elements with different abundances, some of them were normalized. The size of the pie diagram demonstrates either the total level of content of one of the elements or their ratios, while the proportions of associated components are expressed as sector size.

CLASSIFICATION AND THE ABUNDANCE OF PRIMARY MELTS OF ALKALI WITHIN-PLATE MAGMATISM.

The compositions of primary magmas reflect the lateral and vertical heterogeneity of mantle protolith and primary trace element specialization. The identification of deep-seated magma generation zones of different composition (petrochemical province) is complicated by a significant change of the primary melts during their complex and multistage evolution. Crystallization differentiation, interaction with host rocks, mixing, and assimilation occur in the oceanic crust and volcanic apparatus at islands and seamounts. The melt that separated from the mantle protolith immediately changes its compositions, and magmas erupted at the surface significantly differ from the primary magmas. Unlike shallow tholeiite melts, alkali magmas were presumably generated at a lower level of the upper mantle and underwent more complex multistage evolution. In our study, only weakly differentiated volcanic rocks were considered to avoid secondary processes.

In our study we used about 3000 analyses, taken from the database on the Atlantic Ocean close to the primary magmas and characterizing 190 occurrences of within-plate magmatism. Seamounts located around the Mid-Atlantic Ridge were excluded (450 analyses) to reduce the effect of mixing between MORB tholeiites and within-plate rocks. In addition, we discarded a few analyses related to aseismic rises (for example, the Walvis Ridge) of an ambiguous nature. Some geologists suggest that they are tectonic rather than volcanic

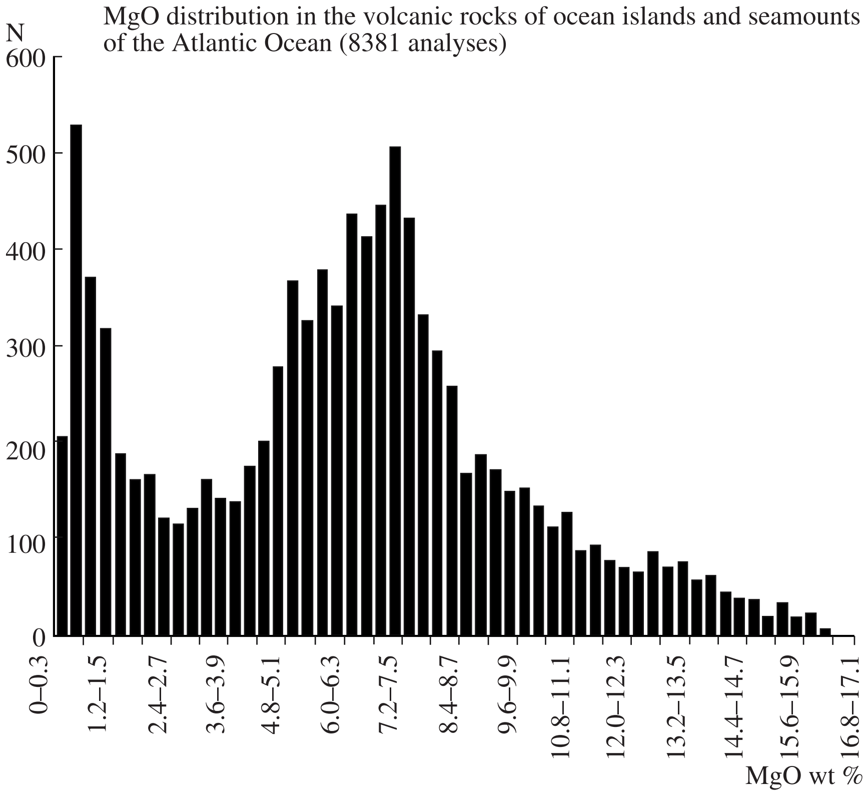

Fig. 1. Histogram of MgO distribution in the within-plate volcanics of the Atlantic Ocean. Sampling involved all volcanic occurrences, Iceland included.

in origin. Thus, the final sampling comprised 2400 analyses.

Primary melts have high Mg/(Mg+Fe) = 0.7–0.8, significant Ni contents and were formed in equilibrium with mantle olivine at a high temperature and pressure [11]. Based on these parameters, we utilized only high-Mg compositions of rocks from ocean islands and seamounts, which have MgO content from 6.8 to 24% and represent olivine-saturated liquid of cotectic composition. It should be taken into account that high-alkali melts have a wide crystallization field of olivine [11]. Therefore, melts with MgO > 24% represent olivine cumulates (heterogeneous olivine–melt systems that aroused from olivine settling) and were rejected. The selected MgO range was justified by our statistical studies. Figure 1 demonstrates a histogram of MgO content within a range from 24 to 0.2%. It is well seen that the main frequency maximum lies at 6.8% MgO. This value corresponds to the most stable association during formation of primary magmas.

To classify the compositions, the data points were plotted in the diagram total alkalis–silica (Fig. 2), which was proposed by Le Bas [12] and proved and modified by the International Commission on Rock Nomenclature [13].

The data points are plotted in four fields: foidites, picrobasalts–picrites, tephrites–basanites, and basalts. In addition, the basalts are subdivided into subalkali and alkali rocks using the Macdonald–Katsura line [14]. Thus, five petrochemical magma types could be distinguished among primary compositions:

(1) Foidites (18%)[*] are low-Si (41% SiO_2) rocks, often with high contents of alkalis and normative olivine (up to 15%). This group involves rocks with normative larnite and modal melilite. Most volcanic rocks have alkali content >4%. The group shows the highest MgO content and contains feldspathoids.

(2) Picrobasalts (ankaramites) account for 7%. They have high MgO contents, low values of normative nepheline (~5%), and occasionally contain normative quartz.

(3) Basanite–tephrites (37%) compose the most representative group and differ from the previous groups in having high total alkalis about 6–8%. This group has high contents of MgO and contains normative nepheline and often also modal nepheline or other fledspathoids. The concentrations of alkalis and MgO show wide variations at a relatively narrow range of SiO_2 (41–45%).

(4) Alkali basalts (24%) are normative nepheline-bearing rocks, which are separated from quartz-norma-

---

[*] Calculated without Iceland tholeiitic basalts.

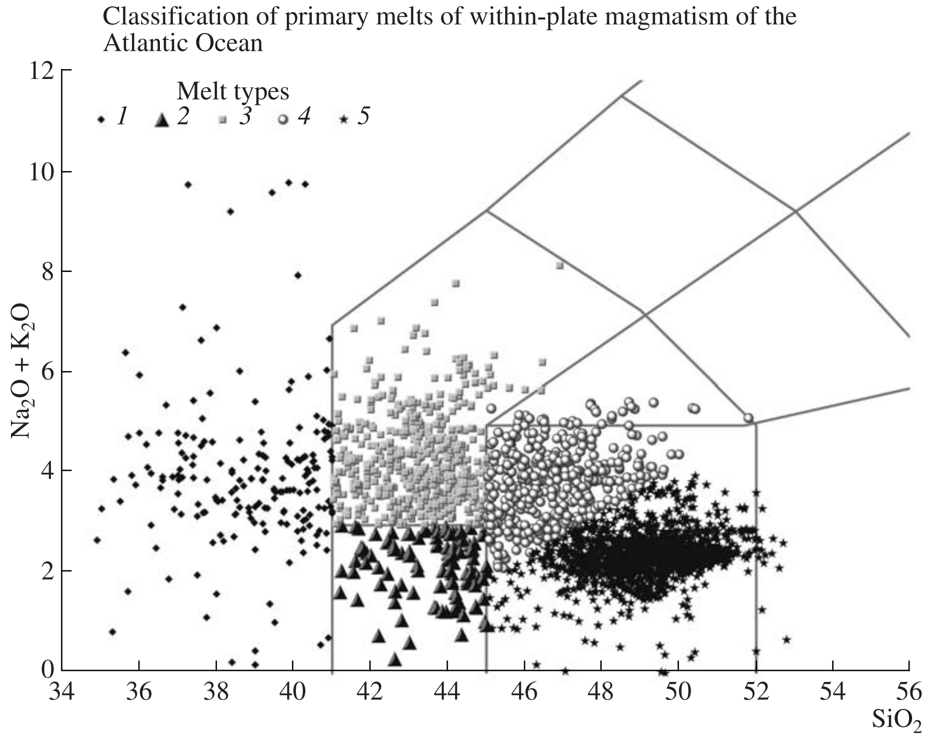

Fig. 2. Positions of data points of primary magmas in the classification diagram for magmatic rocks [12] with an additional line separating the normal and subalkaline basalts ((1) foidites, (2) picrites, (3) basanite, (4) alkali olivine basalts, (5) tholeiites).

tive rocks by the Macdonald–Katsura line [14]. Their major element composition shows a weak dispersion.

(5) Basalts of normal alkalinity, tholeiites (14%). In composition, these are tholeiitic basalts that are quartz–normative rocks or have extremely low contents of normative nepheline. However, these rocks cannot be ascribed to typical ocean floor tholeiites (MORB) according to Hoffman [5]. The rocks of this field are

Table 1. Average compositions of primary melts of the Atlantic Ocean

Component	Foidite (306)*	Picrite (151)	Basanite–nephelinites (892)	Alkali olivine basalts (714)	Tholeiites (1870)
	Average (min–max)	Average (min–max)	Average (min–max)	Average (min–max)	Average (min–max)
SiO_2	38.74 (29.07–40.99)	43.48 (41.2–45)	43.14 (41–46.9)	46.77 (45.07–50.42)	49.08 (45–52.95)
TiO_2	3.77 (0.09–7.23)	2.37 (0.04–5.07)	3.22 (0.05–7.42)	2.58 (0.77–4.72)	1.51 (0–9.7)
Al_2O_3	11.2 (0–18.97)	12.41 (4.97–26.92)	12.89 (2.58–18.9)	13.53 (3.96–19.56)	14.31 (0.97–25.26)
Fe_2O_3	5.95 (0–17.42)	6.11 (0–15.21)	5.82 (0–16.2)	5.18 (0.62–55)	5.13 (0–15.79)
FeO	8.08 (1–15.28)	7.4 (2.1–11.44)	7.86 (1.23–12.78)	8 (0–14)	7.37 (0–12)
MnO	0.21 (0–0.82)	0.17 (0–0.32)	0.18 (0–0.49)	0.18 (0–1.53)	0.15 (0–1.21)
MgO	12.78 (7.04–23.71)	12.55 (7–23.53)	10.64 (7–23.92)	9.87 (7–19.65)	9.08 (7–22.32)
CaO	12.49 (0–22.08)	12.27 (4.22–23.63)	11.1 (0.01–15.87)	10.44 (7.08–14.74)	12.33 (0.37–23.65)
Na_2O	2.67 (0.03–8.5)	1.54 (0.12–3)	3.09 (0.59–17)	2.78 (1.43–4.41)	2.13 (0.02–3.71)
K_2O	1.28 (0.03–10.27)	0.51 (0–1.28)	1.37 (0.36–8.72)	1.12 (0–2.80)	0.24 (0–2.05)
P_2O_5	1.04 (0–3.33)	0.36 (0–1.17)	0.87 (0.04–86)	0.68 (0–97)	0.17 (0–14)

Note: * Number of samples in the set.

shifted toward more felsic compositions, with some points plotting in the field of basaltic andesites.

The sampling is large enough to estimate the proportions and average compositions of the distinguished types of primary melts (Table 1). Our data distinctly highlight the alkalic nature of the Atlantic within-plate magmatism. The primary high-alkali compositions of the first and third types (foidites and basanites) account for about 40% of the primary magmas. The most abundant primary magmas of the Atlantic are basanites, which are followed by alkali basalts, foidites, and picrites.

The abundance of the distinguished types of primary magmas of Atlantic within-plate magmatism is shown in Fig. 3, and the average compositions are shown in Table 1. Owing to the results of a detailed study, data on Iceland tholeiites significantly dominate over tholeiites from other regions [15]. Excluding this magmatic source, we obtained 36 to 24% tholeiites, which reflects the definitely alkali character of Atlantic within-plate magmatism. Primary, high-alkali foidites and alkali basalts account for more than half of the primitive magmas. It should be noted that the estimates proposed for the abundance are based on the sampling frequency rather than on the actual areas of volcanic rocks. Unfortunately, the volumes of different petrochemical types were not calculated, which is the task for future research. However, even approximate estimates are interesting.

The composition of primary melts is plotted on the right-hand branch of the first maximum, within the MgO range of 6.8–24%. Subsequent differentiation occurs in intermediate magmatic chambers, and low-Mg lavas are intermediate differentiates on the way towards pseudoeutectic points that complete the evolution of the magma, the second maximum in the diagram. Two maximums in the frequency distribution plot reflects the classic Daly gap [16], which was first identified in continental igneous rocks. The great abundance of intermediate (about 7% MgO) and end members has no reliable explanation as of yet. The limited abundance of high-Mg melts is presumably determined by the high densities of these liquids [17], which prevent their ascent to the upper structural levels. When considering the dynamics of melt ascent to the surface, many authors [18] distinguish the so-called neutral buoyancy zone, which separates overlying highly porous rocks, which are lighter than magmatic melts, from the underlying heavier rocks [19]. These zones are the most favorable for the formation of intermediate magmatic chambers. According to the calculations [19], these zones are located at depths of about 2–3 km. Experimental data show that volatiles (H_2O and CO_2) significantly decrease the density of aluminosilicate melts owing to the very high mole volumes (tens of cubic centimeters per gas mole). The supply of volatile-

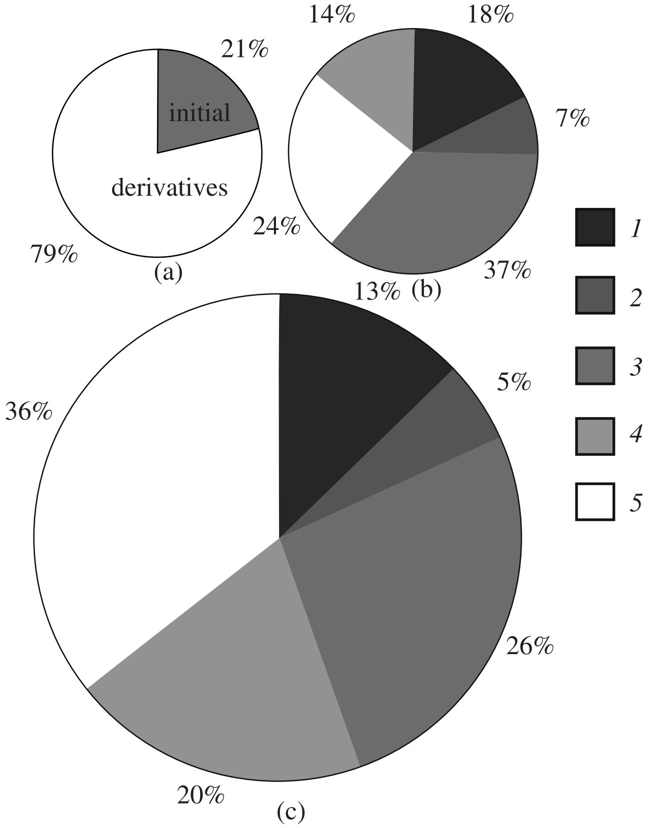

Fig. 3. Melt types in the Atlantic Ocean. (a) proportions of the primary and differentiated melts; (b) abundance of primary magmas (without Iceland); (c) abundance of all occurrences of the Atlantic primary magmas ((1) foidites, (2) picrites, (3) basanites, (4) alkali olivine basalts, (5) tholeiites).

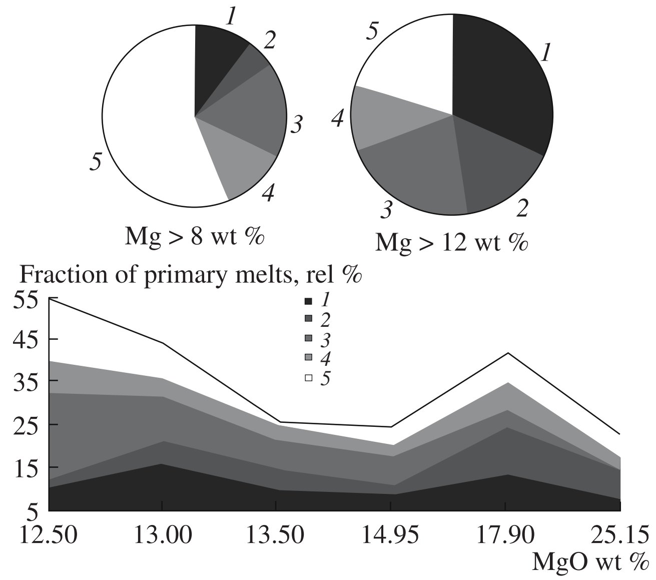

Fig. 4. Variations in the proportions of the five types of primary melts at different MgO contents. Data on Iceland account for 20% of the total sampling and were excluded to obtain an adequate sampling. (*1*) Foidites, (*2*) picrites, (*3*) basanites, (*4*) alkali olivine basalts, (*5*) tholeiites.

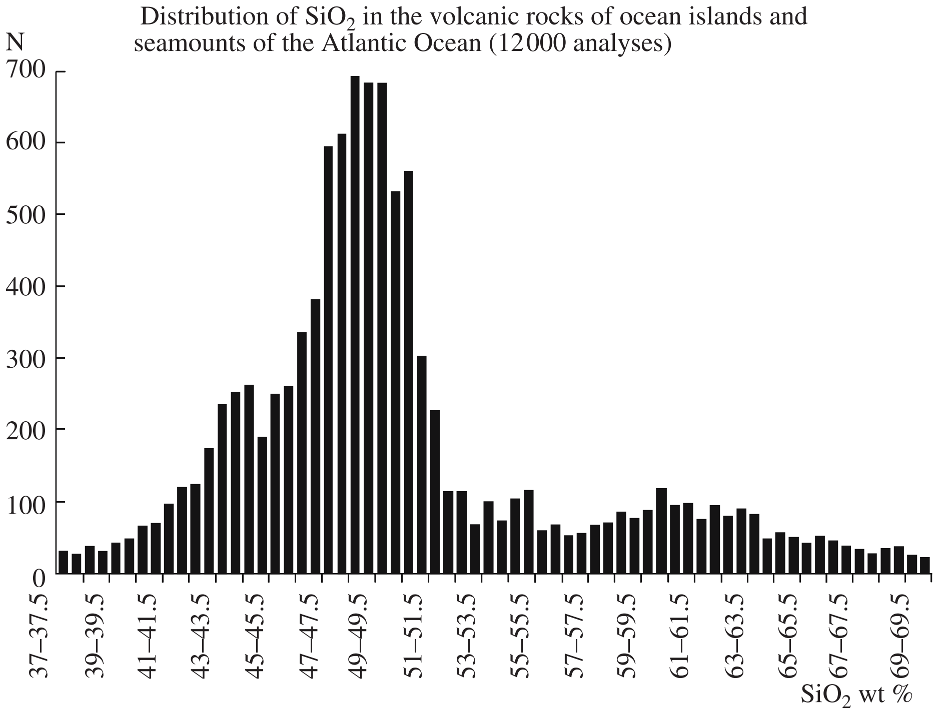

Fig. 5. Histogram of the SiO_2 distribution in the within-plate volcanic rocks of the Atlantic Ocean. Data comprise all occurrences, Iceland included.

rich magmas in these zones could trigger the ascent of the melts and their eruption. For example, the addition of 0.67% H_2O and 0.3% CO_2 to komatiite melt (30% MgO) causes a 5% decrease in its density, and the melt ascends to the surface analogously to a melt containing only 8% MgO.

Detailed analysis of the abundance of high-Mg within-plate magmas (Fig. 4) shows that the higher the Mg content in primary melts, the lower the proportion of tholeiitic rocks. This presumably can be explained by significantly higher volatile contents in alkali melts as compared to those in tholeiitic magmas.

In general, differentiated varieties strongly dominate over primary melts in the Atlantic Ocean (80 and 20%, respectively, Fig. 3). The fact that within-plate alkali magmas of the Atlantic Ocean are dominated by highly differentiated rocks is very interesting and indicates that most primary magmas experienced differentiation in numerous intermediate chambers in the oceanic lithosphere. We also considered the SiO_2 distribution in them (Fig. 5). Unlike two maximums typical of continental magmatism, oceanic alkali rocks demonstrate only one maximum. This distribution can be explained by the fact that felsic differentiated rocks are practically absent from oceanic rocks but are widespread on continents.

The spatial distribution of distinguished types of primary melts in the occurrences is shown in Figs. 6–8. These maps show the types of primary melts of within-plate magmatism in the Atlantic. The pie diagrams with proportions between different types of primary magmas are shown in each occurrence of primary melt, with the circle size proportional to the total number of the samples.

The analysis of the spatial distribution of persistent associations of different types of primary melts allowed us to recognize the following petrochemical provinces.

(1) North Atlantic Ocean (Iceland, Faeroe Islands, Jan Mayen Island). The province is characterized by the predominance of basaltic (elevated alkalinity) and tholeiitic varieties (fourth and fifths types of primary magmas), in the almost complete absence of foidites but widespread picrites.

(2) Central and West Atlantic at the latitude of 30°S, which includes the Azores Archipelago, New England seamounts, Madeira Island, and nearby seamounts. These areas demonstrate a high magmatic activity, with limited tholeiitic magmatism and primary melts mainly ascribed to type 4 of alkali basalts. The Azores Archipelago shows a systematic eastward increase in the abundance of alkali basanite–tephrite melts of the third type and a decrease in alkali basaltic melts.

(3) A province comprising the western African coast, the Cape Verde Islands, the Canary Archipelago, and the Cameroon line. The primary magmas of this area are characterized by a wide spectrum of alkali magmatism, with the predominance of basanite–tephrite and alkali basaltic magmas and insignificant amounts (if any) of tholeiitic melts. The island arc chain

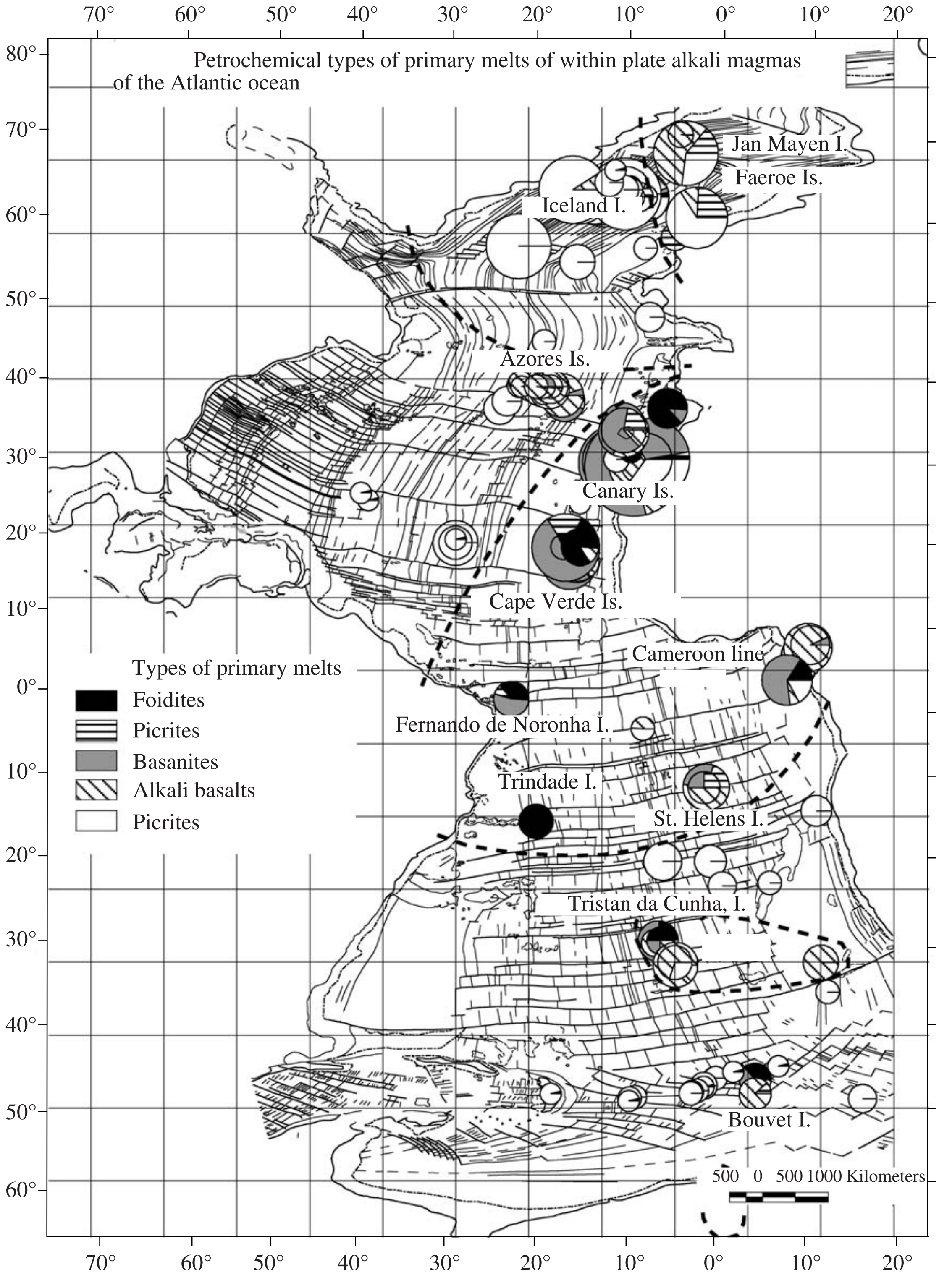

Fig. 6. Map of the petrochemical types of within-plate primary melts of Atlantic alkali magmatism.

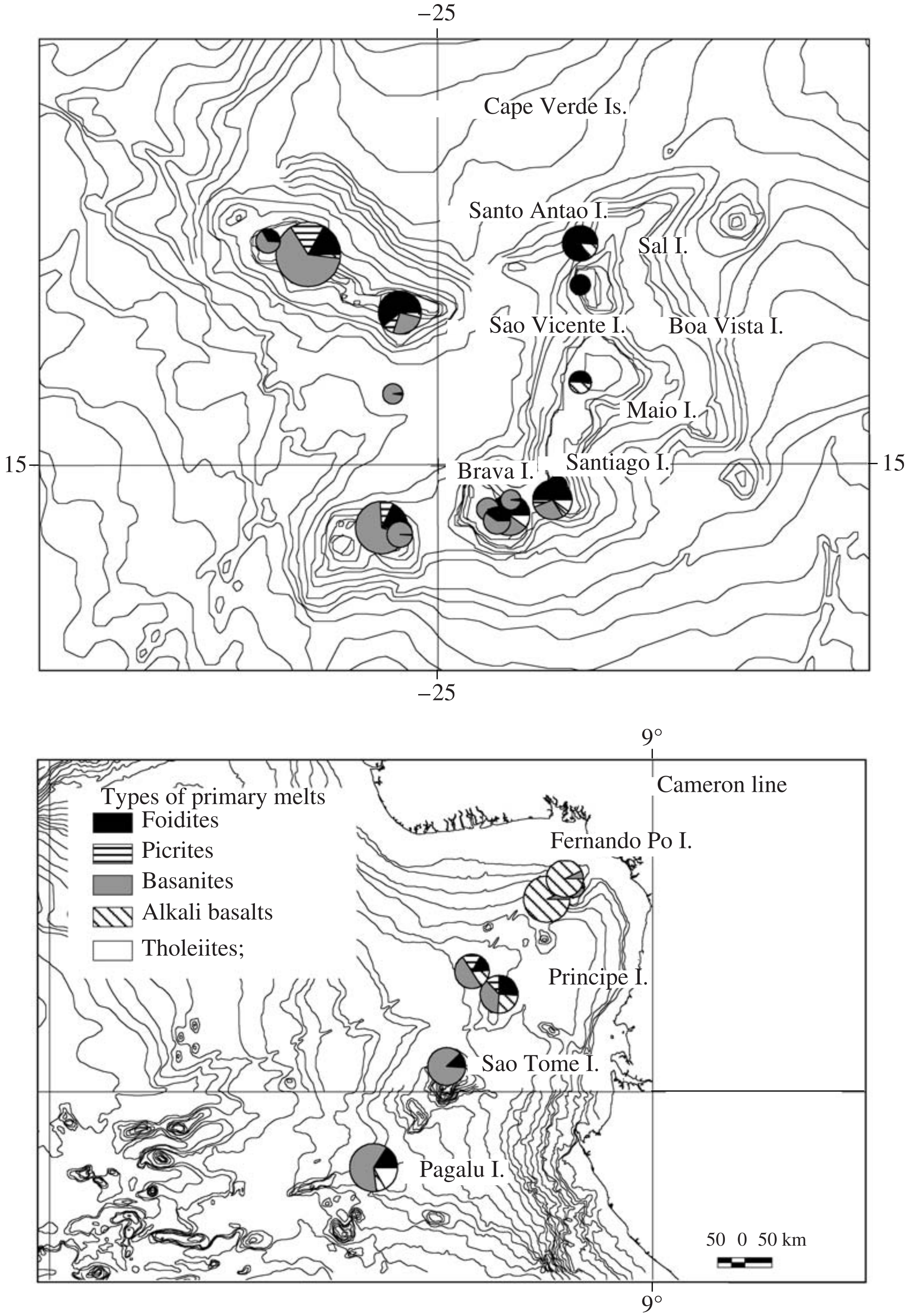

Fig. 7. Map of the petrochemical types of volcanic rocks in the Cape Verde Islands and Cameron line.

of the Cameroon line shows a distinct zoning, with oceanward change from alkali basaltic magmatism to the higher alkali foidite and basanite–tephrite melts. The Canary Archipelago and Cape Verde Islands demonstrate a more complex internal zoning (Fig. 8).

(4) The eastern coast of South America. The primary melts mainly belong to the first petrochemical type, foidite. The Fernando de Noronha Islands, in addition, are abundant in basanite–tephrite primary melts. Tholeiitic and alkali basaltic compositions are absent.

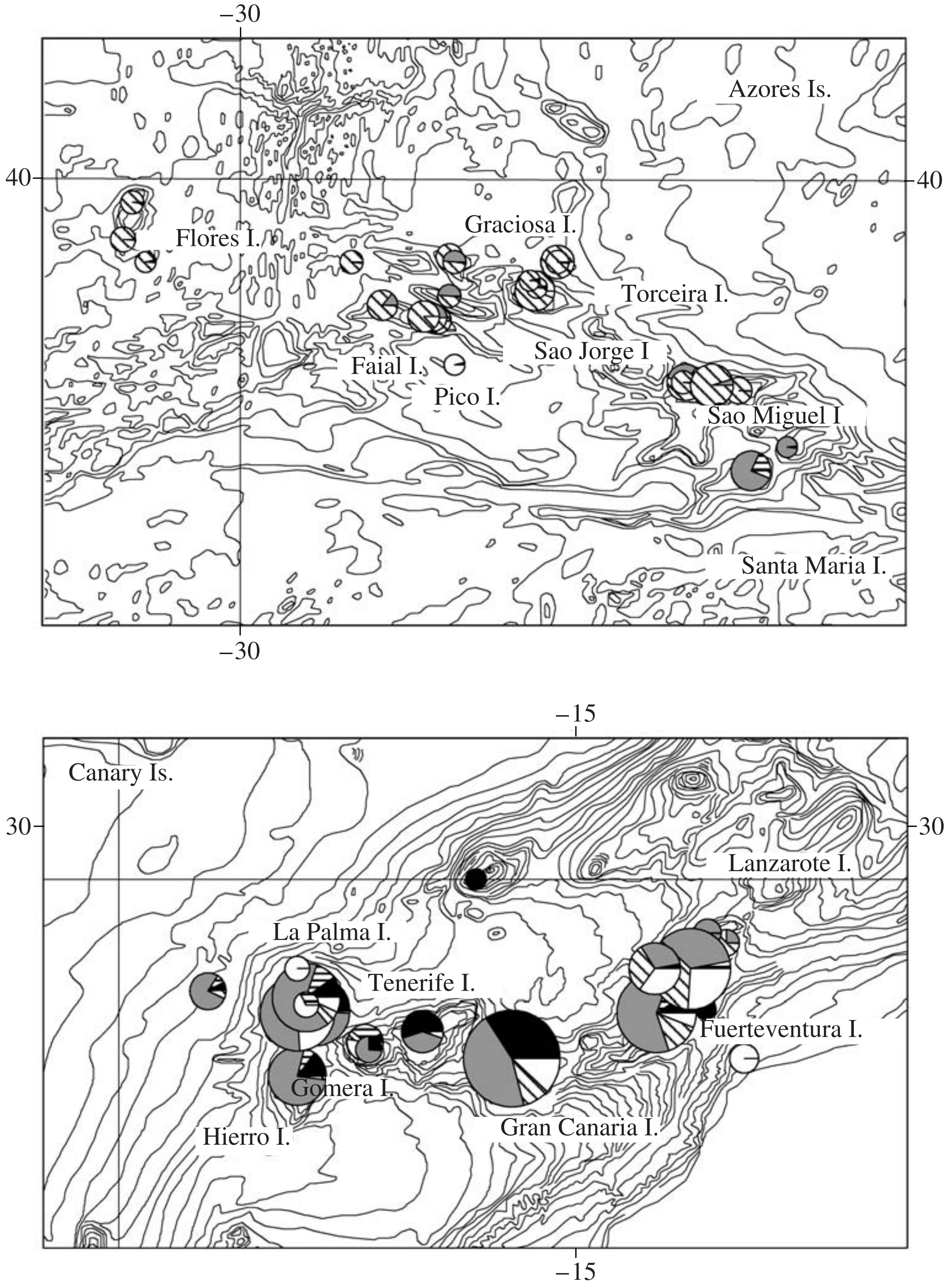

Fig. 8. Map of the petrochemical types of volcanic rocks of the Azores and Canary archipelagos (see Fig. 6 for symbol explanations).

(5) Magmatism of seamounts in the Walvis Ridge and Ascension Island are characterized by the tholeiitic melts with subordinate alkali basalt.

(6) South Atlantic Ocean, the 40s S latitudes, including Gough, Tristan da Cunha, St. Helens Islands. The islands are dominated by basaltic magmatism, which occasionally associates with foidites and basanites. The primary melts of Tristan da Cunha island are characterized by elevated K content.

(7) The Antarctic segment is characterized exclusively by the fifth type of magmatism.

The following conclusions can be drawn.

1. Primary magmas of within-plate magmatism comprise five major types (listed in order of their

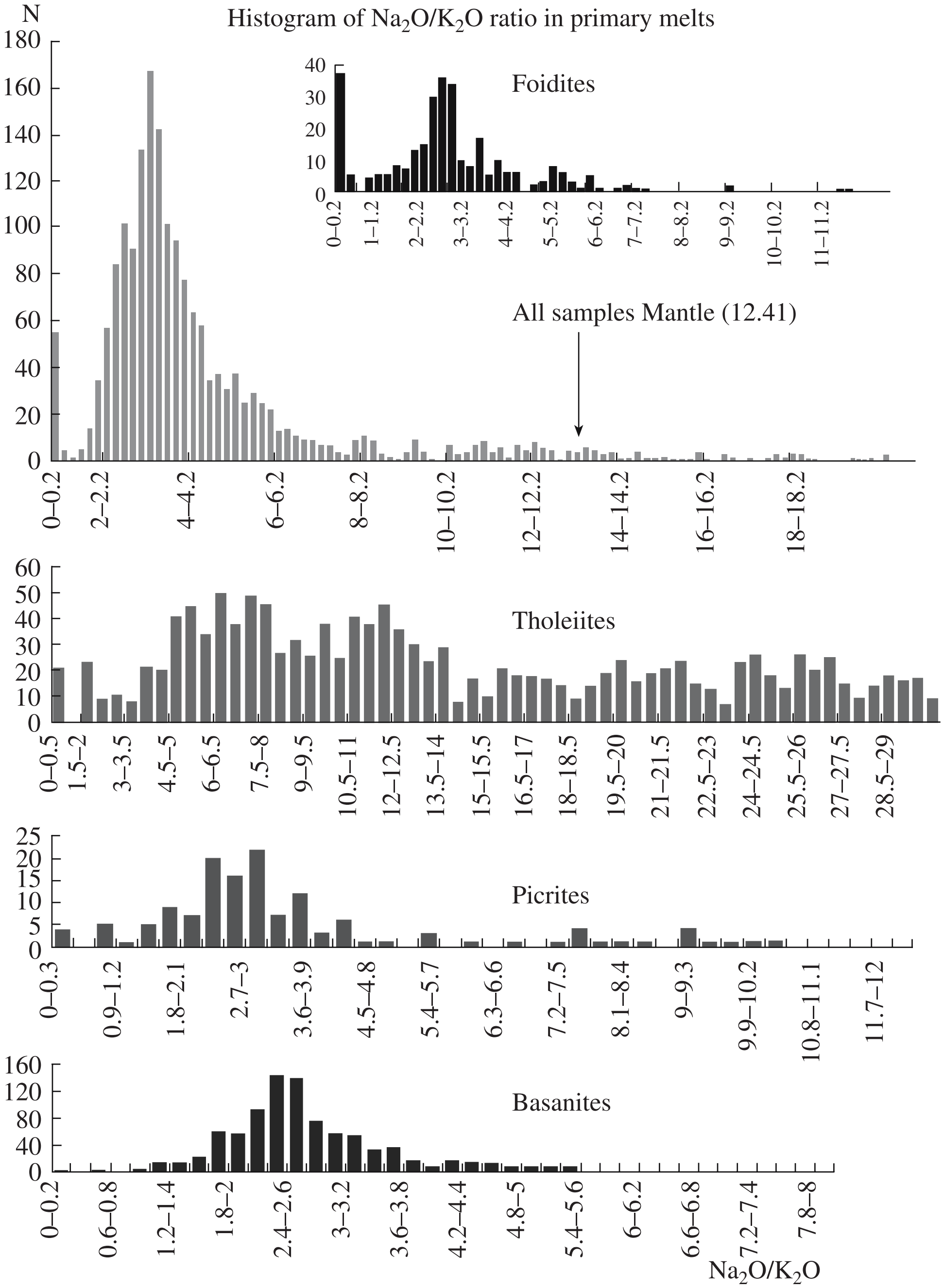

Fig. 9. Variations of Na_2O/K_2O ratios in the primary melts of Atlantic within-plate magmatism for different types of primary magmas and for the whole sampling.

decreasing abundances): tholeiites, basanite tephrites, alkali basalts, foidites, and picrites.

2. Within-plate magmatism of the Atlantic Ocean shows spatial zoning. Zones with the predominance of weakly alkaline tholeiitic magmatism give way to zones with the predominance of alkali types of magmas: basanite–tephrite and foidites.

3. The distribution of magma types within local structures is not related to the position of MOR and other tectonic structures and presumably attests to the deeper-seated generation of within-plate magmas.

TYPOMORPHIC ELEMENTS OF THE FORMATION OF PRIMARY WITHIN-PLATE MAGMAS

It is known that the alkalinity of natural magmas is determined mainly by the total alkalis and SiO_2 content. This testifies that the total alkalinity of primary within-

Table 2. Examples of high-K primary melts of the Atlantic Ocean

Component	Cameroon line		Canary Islands				Cape Verde Islands		St. Helens Island
	Location								
	Pagalu (Annobon) Island	Sao Tome I.	Gran Canaria I.	Gran Canaria I.	Gran Canaria I.	Teneriphe I.	Maio I.	Maio I.	St. Helens Island
SiO_2	38.36	42.26	39.87	40.3	39.44	37.26	40.11	40.11	46.9
Al_2O_3	4.95	2.17	5.07	6.42	6.13	6.56	1.53	1.53	1.08
TiO_2	15.06	15.55	11.9	12.37	12.09	15.54	13.91	13.91	18.9
Fe_2O_3	–	1.63	–	–	–	–	5.09	5.09	–
FeO	11.16	9.92	–	–	–	–	10.08	10.08	3.65
MnO	0.82	–	0.37	0.31	0.34	0.18	0.2	0.2	0.03
CaO	15.64	10.4	18.74	17.67	16.71	12.72	11.59	11.59	7.61
MgO	0.01	4.93	0	0	0.05	–	5.21	5.21	1.93
Na_2O	0.75	0.84	1.4	1.38	0.92	1.22	1.51	1.51	1
K_2O	8.53	6.25	8.46	8.45	8.74	8.6	6.49	6.49	7.2
N_2O/K_2O	0.09	0.13	0.17	0.16	0.11	0.14	0.23	0.23	0.14
Total	95.28	93.95	85.81	86.9	84.42	82.08	95.72	95.72	88.3
Reference	[23]	[24]	[25]			[26]	[27]		[28]

plate magmas of the Atlantic increases in a series of tholeiite, alkali basalts, picrites, basanite, and foidites. The Ti and P contents and K/Na ratios increase in this series also.

As is seen in the histogram of the Na_2O/K_2O ratio (Fig. 9), the majority of oceanic melts can be classed with Na magmatism. At the same time, the small maximum makes it possible to distinguish a group with elevated K contents ($Na_2O/K_2O < 1.2$). At an average mantle value of 12.4 [20], the compositions of Atlantic within-plate magmatic rocks are shifted towards the more potassic composition. In particular, the alkali within-plate magmas of the Atlantic Ocean are characterized by $Na_2O/K_2O = 2–3$, which suggests a fairly high Na melt/residue partition coefficient during the partial melting of the Atlantic mantle, whereas K should intensely enrich the melt owing to low partition coefficients (<1). In high-pressure fields, Na is dissolved in mantle clinopyroxenes as the jadeite end member ($NaAlSi_2O_6$), and its content in the deep-seated clinopyroxenes can be as high as a few percent. Experimental data show that the Na partition coefficient for clinopyroxenes significantly increases from 0.1 at atmospheric pressure to 0.8 at a pressure of 50 kb. This tendency is preserved up to at least 8 GPa (up to $K_{Na} \sim 1.3$). At depths of more than 450 km, all clinopyroxene with Na is dissolved in majorite garnet. When garnet is transformed into the perovskite structure, Na is incorporated mainly in calcium perovskite. Data on alkali distribution in primary magmas unambiguously indicate significant fractionation of K relative to Na. As compared to Na, K more efficiently goes into the melt. A small group of K melts (Table 2) with ($Na_2O/K_2O = 1.2$) is distinguished among K melts. Very interesting tendencies were revealed by the GIS-based compilation of the map of the abundances of Atlantic high-K magmas ($Na_2O< K_2O< 1.2$) (Fig. 10). It is seen that potassic rocks are present in practically all occurrences of oceanic magmatism. High-K primary rocks are confined to the zones with the thickest oceanic lithosphere, which suggests that potassic magmas are the deepest-seated primary melts of the Atlantic (Cape Verde Islands, Canary Archipelago, St. Thomas, seamounts of the Cameroon line). High-K continental rocks (lamproites, leucite alkali basalts, and others) are typically regarded as derived by the melting of the phlogopite-bearing highly metasomatized mantle [21]. The study of microinclusions in diamonds [22] and mineral assemblages of metasomatized mantle nodules supports the existence of carbonate and silicate melt–fluid significantly enriched in alkalis and especially K at large depths. For instance, diamond fluid-bearing microinclusions from Botswana contain, according to Navon [29], 18.1–21.4% K_2O and only 2.2–3.0% Na_2O. The discovery of mantle clinopyroxenes with up to 4.67% K_2O also supports the existence of these melts–fluids.

It is interesting to consider the Ti distribution in Atlantic primary melts (Fig. 11). The histogram demonstrates a systematic change in the Ti content of various types of primary melts, at a wide range of its contents, especially for foidites, picrites, and basanites.

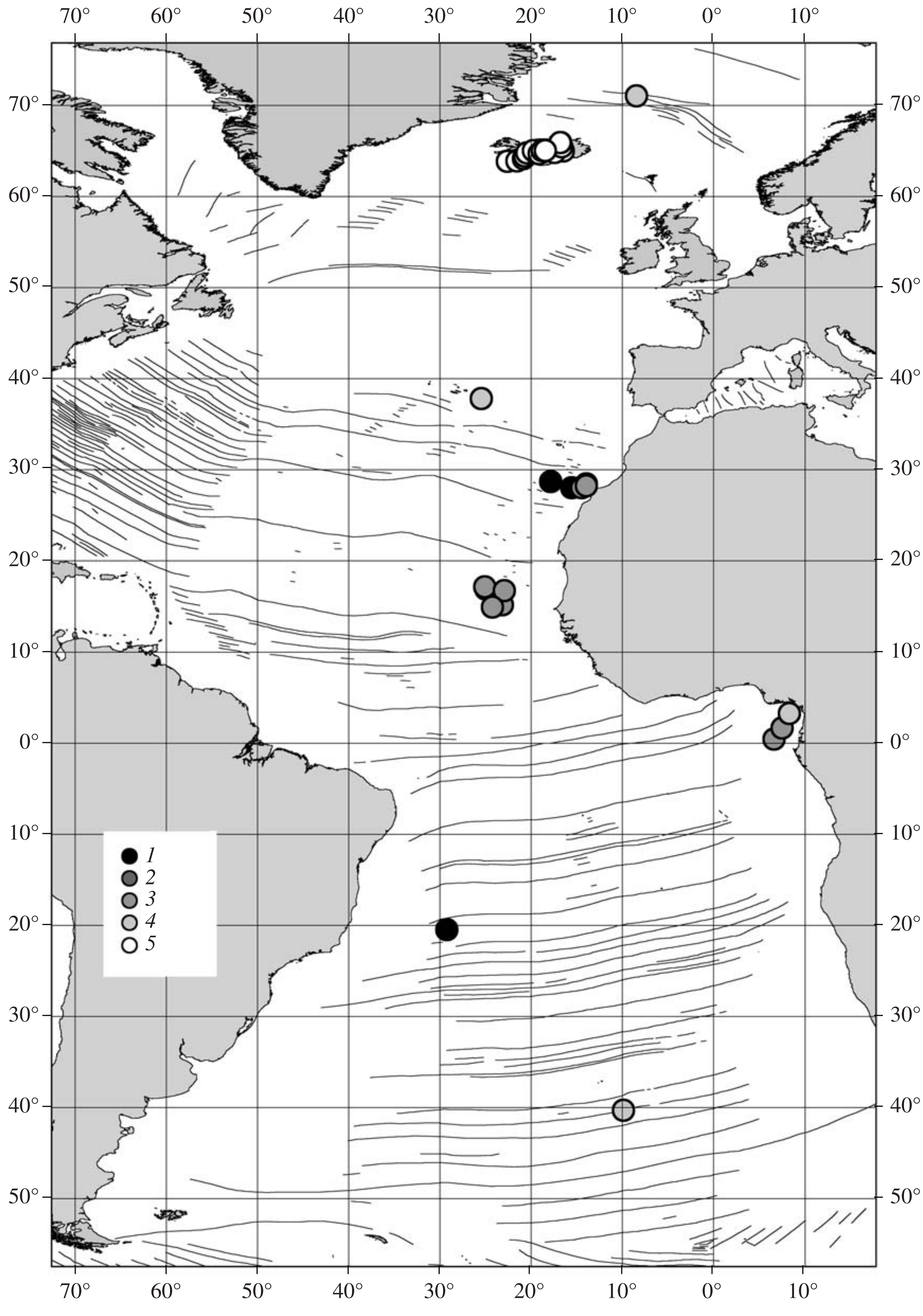

Fig. 10. Map of the occurrences of the high-K primary melts ($Na_2O/K_2O < 1.2$). (1) Foidite, (2) picrite, (3) basanite, (4) alkali basalt, (5) tholeiite.

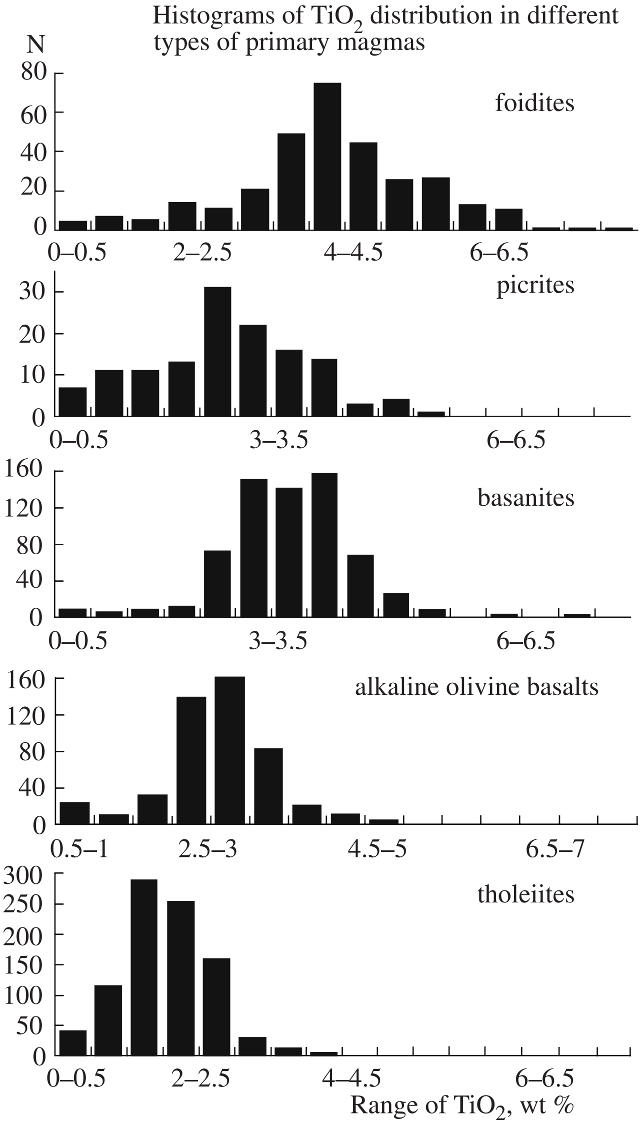

Fig. 11. Histogram of TiO_2 distribution in the within-plate volcanic rocks of the Atlantic Ocean. Data were compiled for all of the occurrences.

The Ti content increases with increasing alkalinity of primary magmatic melts. The highest alkali rocks, foidites, have an average TiO_2 content of 3.85%. This distribution is consistent with the experimental data [30], which demonstrated an increase in the Ti solubility with increasing alkalinity. This indicates that alkali melts more efficiently extract Ti than other melts do, all other conditions being equal. It should be noted that the Ti content in foidites significantly exceeds the highest Ti contents for pyrolite solidus, which accounts for ~3%, according to experimental data [31]. Hence, these magmas could not melt directly from the peridotite mantle. The introduction of Ti and, presumably, K into the deep-seated magma generation zones was presumably related to mantle metasomatism. As follows from numerous lines of evidence, Ti is efficiently transported by deep-seated metasomatic, mainly alkali–silicate, melts. Such Ti carriers as rutile, armalcolite, ilmenite, lindsleyite are thought to be the main metasomatic mantle phases [32].

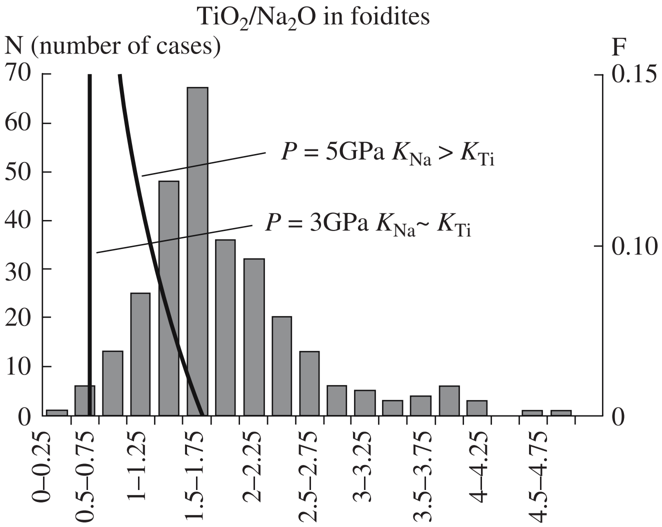

Fig. 12. Variations in the TiO_2/Na_2O ratio of the melt during the melting of garnet lherzolite compositionally close to MORB pyrolite [37]. At pressures of up to 3 GPa, the Na and Ti combined coefficients are close and the TiO_2/Na_2O ratio practically does not depend on the degree of melting and corresponds to that in the primary lherzolite [38]. At high pressures, the partition coefficient of Na significantly increases, while that of Ti slightly decreases, which leads to a significant increase in the TiO_2/Na_2O ratio at a low melting degree. The range of TiO_2/Na_2O ratios is shown for foidites of the Atlantic Ocean.

The Na partition coefficient between clinopyroxene and melt significantly increases with increasing pressure, while the Ti partition coefficient simultaneously decreases with increasing temperature [33] and mole fraction of the enstatite end member in pyroxene [34, 35] (Fig. 12). This makes it possible to use the Ti/Na ratio as an efficient barometer of mantle magma formation [30, 36]. At 3 GPa, the Na and Ti combined partition coefficients at mantle melting are nearly identical and equal to 0.1. Under such conditions, the TiO_2/Na_2O ratio remains approximately similar to that in the source (0.4–0.6 for MORB pyrolite), regardless of the degree of melting [37]. At 5 GPa, their behavior becomes different: K_{Ti} decreases approximately to 0.07, while K_{Na} increases to 0.22. In this case, the TiO_2/Na_2O ratio could increase to 1.3 at extremely low degrees of melting and to 0.7 at 15% melting. Magmas with high ratios (1.4–1.5) can form even under high pressures, because K_{Na} continues to increase to at least 7.5 GPa (Fig. 12). The comparison of experimental data with the TiO_2/Na_2O ratios in the primary magmas of the Atlantic shows that alkali magmas were generated at high depths (TiO_2/Na_2O varies within 0.95–1.53) compared to those of tholeiites (TiO_2/Na_2O ~ 0.7). The

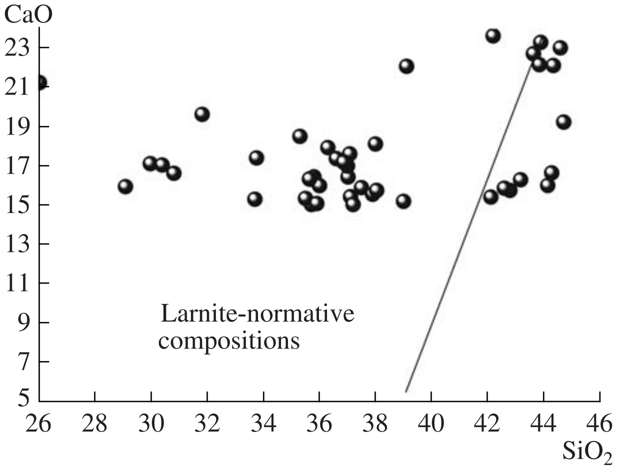

Fig. 13. Distribution of the data points of primary melts in the SiO$_2$/CaO diagram. The line separates larnite-normative and usual compositions [39].

deepest seated melts are foidites and picrites (>200 km).

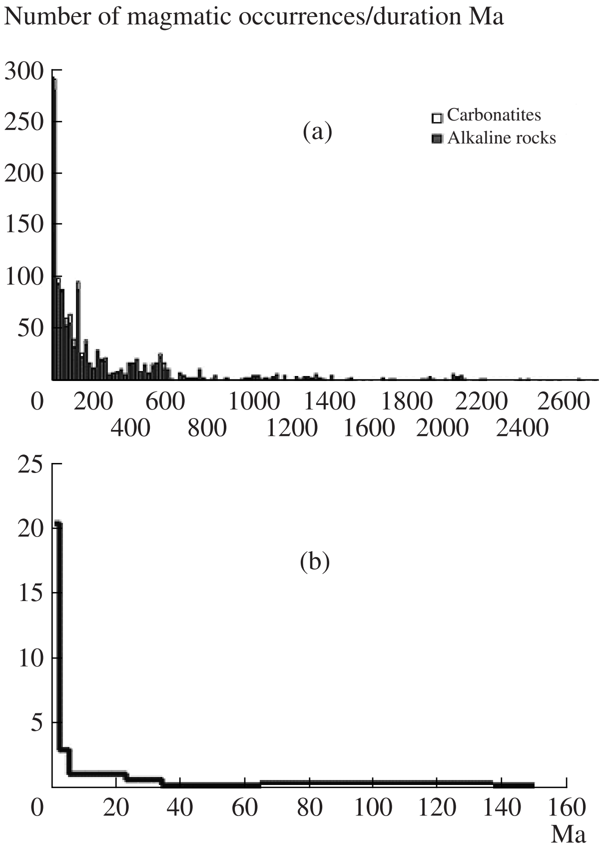

Fig. 14. Temporal change in the activity of alkali magmatism. (a) Continental intrusive alkali magmatism; (b) alkali within-plate magmatism of the Atlantic Ocean [42].

High-Ca rocks ascribed mainly to foidite groups were identified among primary magmas of the Atlantic. The Ca content in these melts is higher than 15%, while the SiO$_2$ content is extremely low, <43%. A previously developed criterion to distinguish the larnite-normative compositions [39] allowed us to identify strongly Si-undersaturated high-Ca rocks (Fig. 13). These rocks comprise mainly olivine melilite-bearing nephelinites. Note that high-Ca magmatism is typical of ocean islands formed in areas with the thickest lithosphere, at flanks of the Atlantic (Canary Archipelago, Cape Verde Islands, Trindade, Fernando da Noronha) (Table 3, Fig. 13). Our experimental data [40] show that high-Ca rocks could not be produced in the course of partial melting of the primitive or MORB-type mantle. Similar melts could result from carbonate mantle metasomatism, which is widespread in the South Atlantic [41]. The evolution of carbonatite volcanism at the Cape

Table 3. Examples of high-Ca primary melts of the Atlantic Ocean

Component	1	2	3	4	5	6	7	8	9	10	11	12	13	14
SiO$_2$	36.6	35.64	35.3	33.69	31.81	36.3	35.5	35.9	36.86	37.11	37.2	35.71	37.02	37.08
Al$_2$O$_3$	9.99	10.34	7.39	11.21	5.86	9.81	9.66	9.45	8.98	9.91	11.24	10.91	9.47	10.25
TiO$_2$	3.25	3.91	6	5.61	6.02	3.07	3.57	3.57	3.3	2.64	3.5	3.09	3.38	2.7
Fe$_2$O$_3$	12.1	13.25	12.13	6.19	13.17	12.92	6.45	5.79	4.92	4.89	5.03	9.72	1.4	1.27
FeO	–	–	6.88	8.35	8.19	–	7.14	7.55	6.28	6.35	6.72	0.68	10.12	9.16
MnO	0.19	0.26	0.17	0.18	0.2	0.18	0.31	0.23	0.19	0.2	0.2	0.17	0.19	0.19
CaO	17.38	16.34	18.51	15.31	19.63	17.94	15.35	15.09	17.2	15.44	15.04	15.04	16.44	17.62
MgO	14.41	10.25	10.82	12.06	11.73	7.6	13.86	14.27	14.25	14.01	11.9	12.94	14.81	13.71
Na$_2$O	3.16	4.35	0.66	1.77	0.6	1.7	2.38	2.75	2.85	3.24	3.03	2.96	2.53	2.69
K$_2$O	0.81	2.1	0.2	1.35	0.14	1.3	1.1	1.06	1.12	0.72	1.32	1.82	1.38	0.53
P$_2$O$_5$	1.27	2.28	1.22	2.2	2.49	0.55	2.07	2.1	1.29	1.33	1.41	1.76	1.15	1.49
Total	99.16	98.72	99.79	98.46	100.4	99.9	99.55	99.41	99.16	99.25	99.39	94.8	98.36	97.08

Note: (1) Maio Island [43], (2) Sao Antonio Island [43]; (3) Fuerteventura Island. [44]; (4–5) Fuerteventura Island [44]; (6) Mount Amper [45]; (7–8) Gran Canaria I. [46]; (9–11) Maio Island [47]; (12) Sal Island [48]; (13) Maio Island [48].

Verde islands (Santiago, Sao Vicente, and Maio) confirm this conclusion.

Thus, the principal conclusions of this section are as follows:

(1) Primary magmas of elevated alkalinity were formed in the Atlantic on the thick oceanic lithosphere at oceanic margins, at depths of more than 200 km, whereas ocean-island and seamount tholeiites were derived from significantly shallower depths.

(2) Mantle metasomatism (carbonate and alkali-silicate) predated the generation of within-plate alkali magmatism of the Atlantic. Carbonate metasomatism is most abundant in the South Atlantic.

EVOLUTION OF ALKALINE VOLCANISM OF THE ATLANTIC OCEAN

The evolution of alkaline within-plate magmatism in the Atlantic Ocean was considered for the first time within the framework of the next research. Since the number of magmatic occurrences should be normalized to the unit area, the change in the oceanic crust area was calculated. As is seen from Figs. 14a and 14b, the role of alkaline magmatism increased with time, reaching a maximum in recent epochs. Earlier we have demonstrated an analogous trend for continental alkali magmatism.

The appearance of alkali magmatism at the Archean–Proterozoic boundary was related to the change of geodynamic regime (activation of subduction processes and, as a result, the involvement of volatiles in mantle processes and the onset of large-scale metasomatism). As was previously proposed in [49], the activation of alkali magmatism in the Earth's history is related to a change in endogenous geodynamics, the transition to one-layer convection in the mantle owing to secular cooling of the Earth, which, in turn, leads to the subduction of plates to the mantle–core boundary and, in response, to the ascent of large masses of hot material, plume sources, from these depths. Thus, the increasing role of alkali magmatism is related to a sharp increase in the plume activity of this region. The activation of alkaline magmatism occurred mainly in Iceland (Iceland–Greenland plume) and in the Canary and Azores archipelagos (Great African plume).

ACKNOWLEDGMENTS

The study was supported by the Program of the Presidium of the Russian Academy of Sciences "Electronic Earth," Federal Program "World Ocean," theme "The Composition and Structure of the Earth's Crust of the World Ocean: Prediction and Estimate of Mineral Resources" (problems 6, 7, 8), and contract no. 634.2006-GEOKHI.

REFERENCES

1. P. W. Gast, "Trace Element Fractionation and the Origin of Tholeiitic and Alkaline Magma Types," Geochim. Cosmochim. **32**, 1057–1086 (1968).
2. M. Tatsumoto, "Isotopic Composition of Lead in Ocean Basalt and Its Implication to Mantle Evolution," Geotektonika **8**, 6 (1978).
3. W. M. White and A. W. Hofmann, "Sr and Nd Isotope Geochemistry of Oceanic Basalts and Mantle Evolution," Nature **296**, 821–825 (1982).
4. R. D. Van der Hilst and H. Karason, "Compositional Heterogeneity in the Bottom 1000 Kilometers of Earth's Mantle: Toward a Hybrid Convection Model," Science **28**, 1885–1888 (1999).
5. A. W. Hofmann, "Sampling Mantle Heterogeneity Through Oceanic Basalts: Isotopes and Trace Elements," Treatise On Geochemistry **2**, 61–101 (2003).
6. B. Dupre and C. J. Allegre, "Pb–Sr Isotope Variation in Indian Ocean Basalts and Mixing Phenomena," Nature **303**, 142–146 (1983).
7. K. Asch, "The Geological Map :The Visual Language of Geologists (with too Many Dialects for even the most Sophisticated Computers)," in *Proceedings of Conference GIS-in Geology, Moscow, Russia, 2002* (Moscow, 2002), p. 15.
8. V. M. Ryakhovsky, "Methodical Problems of the Integral Analysis of Compositional Variations of the Magmatic Rocks," in *General and Regional Problems of Geology. Formation Dynamics, Structure, Composition, and Mineral Resources of Fold Systems and Sedimentary Basins of Various Geodynamic Settings. Project A.0070 FTsP "Integratsiya"* (GEOS, Moscow, 2000), Vyp. 2, pp. 214–225 [in Russian].
9. V. M. Ryakhovsky, "Evolution of Basaltic Magmatism in the Ocean: A Computer-Aided Study Geodinamic and Metallogeny," in *Theory and Implications for Applied Geology* (Moscow, 2000).
10. *Tectonic Map of the World (Globe). Scale 1:10000000*, Ed. by L. P. Zonenshain, (GosKomNedra, VNIIZarubezhgeologiya, Moscow, 1995) [in Russian].
11. D. H. Green and A. E. Ringwood, "The Genesis of Basaltic Magmas," Contrib. Mineral. Petrol. **15**, 103–190 (1967).
12. M. J. Le Bas and A. L. Streckeisen, "The IUGS Systematics of Igneous Rocks," J. Geol. Soc. London **148**, 825–833 (1991).
13. *Classification of the Magmatic (Igneous) Rocks and Glossary of Terms. Recommendation of Subcommission on Systematics of Igneous Rocks of International Union of Geological Sciences* (Nedra, Moscow, 1997) [in Russian].
14. R. Macdonald, "Nomenclature and Petrochemistry of the Peralkaline Oversaturated Extrusive Rocks," Bull. Volcanol. **38**, 498–516 (1974).
15. *Basaltic Volcanism on the Terrestrial Planets* (Pergamon Press, New York, 1981)
16. R. A. Daly, *Igneous Rocks and the Depths of the Earth*, (McGraw Hill, New York, 1993).
17. E. Stolper and D. Walker, "Melt Density and the Average Composition of Basalt," Contrib. Mineral. Petrol. **74**, 7–12 (1980).

18. A. T. Anderson, "CO_2 and the Eruptibility of Picrite and Komatiite," Lithos **34**, 19–25 (1995).
19. M. P. Ryan, "Neutral Buoyancy and the Mechanical Evolution of Magmatic Systems," in *Magmatic Processes: Physicochemical Principles*, Ed. by B. O. Mysen (Geochem. Soc., New York, 1987), pp. 259–287.
20. W. F. McDonough and S. Sun, "The Composition of the Earth," Chem. Geol. **120**, 223–253 (1995).
21. S. F. Foley, "Vein PlusWall Rock Melting Mechanism in the Lithosphere and the Origin of Potassic Alkaline Magmas," Lithos **28**, 425–453 (1992).
22. N. V. Sobolev and V. S. Shatsky, "Diamond Inclusions in Garnets from Metamorphic Rocks: a New Environment for Diamond Formation," Nature **4**, 742–746 (1990).
23. G. Cornen and R. C. Maury, "Petrology of the Volcanic Rocks of the Island of Annobon, Gulf of Guinea," Mar. Geol. **36**, 253–267 (1980).
24. R. C. Mitchell-Thome, *Geology of the South Atlantic Islands* (Berlin, 1970), pp. 1–350.
25. J. A. Crisp and F. J. Spera, "Pyroclastic Flows and Lavas of the Mogan and Fataga Formations, Tejeda Volcano, Gran Canaria, Canary Islands: Mineral Chemistry, Intensive Parameters, and Magma Chamber Evolution," Contrib. Mineral. Petrol. **96**, 503–518 (1987).
26. V. Arana, J. Marti, A. Aparicio, L. Garcia-Cacho, and R. Garcia-Garcia, "Magma Mixing in Alkaline Magmas: An Example from Tenerife, Canary Islands," Lithos **32**, 1–19 (1994).
27. P. de Paepe, J. Klerkx, J. Hertogen, and P. Plinke, "Oceanic Tholeiites on the Cape Verde Islands: Petrochemical and Geochemical Evidence," Earth Planet. Sci. Lett. **22**, 347–354 (1974).
28. A. A. Abdel-Monem and P. W. Gast, "Age of Volcanism on St. Helena," Earth Planet. Sci. Lett. **2**, 415–418 (1967).
29. O. Navon and E. S. Izraeli, "Cl- and K-Rich Micro-Inclusions in Cloudy Diamonds," EOS, Trans. Am. Geophys. Union **80**, 1128 (1999).
30. K. Putirka, M. Johnson, R. Kinzler, et al., "Thermobarometry of Mafic Igneous Rocks Based on Clinopyroxene–Liquid Equilibria, 0–10 Kbar," Contrib. Mineral. Petrol. **12**, 92–108 (1996).
31. M. J. Walter, "Melting of Garnet Peridotite and the Origin of Komatiite and Depleted Lithosphere," J. Petrol. **9**, 29–60 (1998).
32. M. A. Menzies and C. J. Hawkesworth, *Mantle Metasomatism*, (Acad. Press, London, 1987).
33. J. Adam and T. H. Green, "The Effects of Pressure and Temperature on the Partitioning of Ti, Sr and REE between Amphibole, Clinopyroxene and Basanitic Melts," Chem. Geol. **117**, 219–233 (1994).
34. W. E. Gallahan and R. L. Nielsen, "The Partitioning of Sc, Y, and the Rare Earth Elements between High-Ca Pyroxene and Natural Mafic to Intermediate Lavas at 1 Atmosphere," Geochim. Cosmochim. Acta **56**, 2387–2404 (1992).
35. L. M. Forsythe, R. L. Nielsen, and M. R. Fisk, "High-Field-Strength Element Partitioning Between Pyroxene and Basaltic to Dacitic Magmas," Chem. Geol. **117**, 107–125 (1994).
36. K. Putirka, "Garnet + Liquid Equilibrium," Contrib. Mineral. Petrol. **11**, 27–288 (1998).
37. D. H. Green and T. J. Falloon, "Pyrolite: A Ringwood Concept and Its Current Expression," in *The Earth'S Mantle: Composition, Structure, and Evolution*, Ed. by I. Jackson (Cambridge Univ., Cambridge, 1998), pp. 311–378.
38. A. V. Girnis, V. K. Bulatov, and G. P. Brey, "Primary Magmas of the High-Magnesia Basalts of Mauna Kea Volcano, Hawaii: An Experimental Study," Geokhimiya, No. 4, 366–379 (2003) [Geochem. Int. **41**, 324–337 (2003)].
39. L. N. Kogarko, "Upper Mantle Heterogeneity and Composition of the Primary Magmas of Oceanic Islands," Geol. Geofiz., No. 7, 74–80 (1986).
40. L. N. Kogarko and D. Green, "Phase Equilibria during the Melting of Melilite Nephelinite under Pressures of up to 60 kbar," Dokl. Akad. Nauk **359** (4), 522–524 (1998) [Dokl. Earth Sci. **359**, 404–405 (1998)].
41. L. N. Kogarko, G. Kurat, and T. Ntaflos, "Carbonate Metasomatism of the Oceanic Mantle beneath Fernando de Noronha Island, Brazil," Contrib. Mineral. Petrol. **140**, 577–587 (2001).
42. V. A. Zaitsev, "Evolution of the Activity of Within-Plate Magmatism of the Atlantic Ocean," in *Geochemistry, Ore Potential, and Genesis of Within-Plate Magmatism of the World Ocean, 2002*, pp. 6–12.
43. G. R. Davies, M. J. Norry, D. C. Gerlach, and R. A. Cliff, *A Combined Chemical and Pb–Sr–Nd Isotope Study of the Azores and Cape Verde Hotspots: The Geodynamic Implications,* in *Magmatism in the Ocean Basins*, Ed. by A. D. Saunders and M. J. Norry (Blackwell, Oxford, 1989), pp. 231–255.
44. A. Ahijado and A. Hernandez-Pacheco, "The Ultramafic Alkaline Rocks of Jable de la Salinas, Fuerteventure, Canary Islands," Rev. Soc. Geol. Espana **3**, 275–287 (1990).
45. J. Geldmacher and K. A. Hoernle, "The 72 Ma Geochemical Evolution of the Madeira Hotspot (Eastern North Atlantic): Recycling of Paleozoic (<500 Ma) Oceanic Lithosphere," Earth Planet. Sci. Lett. **183**, 234 (2000).
46. E. Ibarrola and J. Martorell, "Olivine Melilitites of Gran Canaria, Derivatives of an Alkali Basalt Magma," Estud. Geol. (Madrid) **29**, 319–324 (1973).
47. J. Klerkx, S. Deutsch, and P. de Paepe, "Rubidium, Strontium Content and Strontium Isotopic Composition of Strongly Alkalic Basaltic Rocks from the Cape Verde Islands," Contrib. Mineral. Petrol. **45**, 107–118 (1974).
48. A. O. Mazarovich, D. I. Frikh-Kar, L. N. Kogarko, et al., *Tectonics and Magmatism of Cape Verde Islands* (Nauka, Moscow, 1990).
49. L. N. Kogarko and V. E. Khain, "Alkaline Magmatism in the Earth's History: A Geodynamic Interpretation," Dokl. Akad. Nauk **377**, 677–679 (2001) [Dokl. Eart. Sci. **377A**, 359–361 (2001)].